An ultra-fast fiber optic pressure sensor for blast event measurements

2012 Meas. Sci. Technol. 23 055102

(http://iopscience.iop.org/0957-0233/23/5/055102)

Report Documentation Page

Form Approved
OMB No. 0704-0188

1. REPORT DATE	2. REPORT TYPE	3. DATES COVERED
2012		**00-00-2012 to 00-00-2012**

4. TITLE AND SUBTITLE	5a. CONTRACT NUMBER
An Ultra-fast Fiber Optic Pressure Sensor For Blast Event Measurements	5b. GRANT NUMBER
	5c. PROGRAM ELEMENT NUMBER
6. AUTHOR(S)	5d. PROJECT NUMBER
	5e. TASK NUMBER
	5f. WORK UNIT NUMBER
7. PERFORMING ORGANIZATION NAME(S) AND ADDRESS(ES) **US Army Natick Soldier Research,Development & Engineering Center,Natick,MA,01760**	8. PERFORMING ORGANIZATION REPORT NUMBER
9. SPONSORING/MONITORING AGENCY NAME(S) AND ADDRESS(ES)	10. SPONSOR/MONITOR'S ACRONYM(S)
	11. SPONSOR/MONITOR'S REPORT NUMBER(S)

12. DISTRIBUTION/AVAILABILITY STATEMENT
Approved for public release; distribution unlimited

13. SUPPLEMENTARY NOTES
Measurement Science and Technology Volume 23 Number 5, 1/20

14. ABSTRACT

Soldiers who are exposed to explosions are at risk of suffering traumatic brain injury (TBI). Since the causal relationship between a blast and TBI is poorly understood, it is critical to have sensors that can accurately quantify the blast dynamics and resulting wave propagation through a helmet and skull that are imparted onto and inside the brain. To help quantify the cause of TBI, it is important to record transient pressure data during a blast event. However,very few sensors feature the capabilities of tracking the dynamic pressure transients due to the rapid change of the pressure during blast events, while not interfering with the physical material layers or wave propagation. In order to measure the pressure transients efficiently, a pressure sensor should have a high resonant frequency and a high spatial resolution. This paper describes an ultra-fast fiber optic pressure sensor based on the Fabry?Perot principle for the application of measuring the rapid pressure changes in a blast event. A shock tube experiment performed in US Army Natick Soldier Research, Development and Engineering Center has demonstrated that the resonant frequency of the sensor is 4.12 MHz, which is relatively close to the designed theoretical value of 4.113 MHz. Moreover, the experiment illustrated that the sensor has a rise time of 120 ns, which demonstrates that the sensor is capable of observing the dynamics of the pressure transient during a blast event.

15. SUBJECT TERMS

16. SECURITY CLASSIFICATION OF:			17. LIMITATION OF ABSTRACT	18. NUMBER OF PAGES	19a. NAME OF RESPONSIBLE PERSON
a. REPORT	b. ABSTRACT	c. THIS PAGE			
unclassified	**unclassified**	**unclassified**	**Same as Report (SAR)**	**8**	

Meas. Sci. Technol. **23** (2012) 055102 (7pp) doi:10.1088/0957-0233/23/5/055102

An ultra-fast fiber optic pressure sensor for blast event measurements

Nan Wu[1], Xiaotian Zou[2], Ye Tian[1], John Fitek[3], Michael Maffeo[3], Christopher Niezrecki[4], Julie Chen[4] and Xingwei Wang[1]

[1] Department of Electrical and Computer Engineering, University of Massachusetts Lowell, 1 University Ave, Lowell, MA 01854, USA
[2] Department of Biomedical Engineering and Biotechnology, University of Massachusetts Lowell, 1 University Ave, Lowell, MA 01854, USA
[3] US Army Natick Soldier Research, Development & Engineering Center, Natick, MA 01760, USA
[4] Department of Mechanical Engineering, University of Massachusetts Lowell, 1 University Ave, Lowell, MA 01854, USA

E-mail: xingwei_wang@uml.edu

Received 4 November 2011, in final form 12 March 2012
Published 11 April 2012
Online at stacks.iop.org/MST/23/055102

Abstract
Soldiers who are exposed to explosions are at risk of suffering traumatic brain injury (TBI). Since the causal relationship between a blast and TBI is poorly understood, it is critical to have sensors that can accurately quantify the blast dynamics and resulting wave propagation through a helmet and skull that are imparted onto and inside the brain. To help quantify the cause of TBI, it is important to record transient pressure data during a blast event. However, very few sensors feature the capabilities of tracking the dynamic pressure transients due to the rapid change of the pressure during blast events, while not interfering with the physical material layers or wave propagation. In order to measure the pressure transients efficiently, a pressure sensor should have a high resonant frequency and a high spatial resolution. This paper describes an ultra-fast fiber optic pressure sensor based on the Fabry–Perot principle for the application of measuring the rapid pressure changes in a blast event. A shock tube experiment performed in US Army Natick Soldier Research, Development and Engineering Center has demonstrated that the resonant frequency of the sensor is 4.12 MHz, which is relatively close to the designed theoretical value of 4.113 MHz. Moreover, the experiment illustrated that the sensor has a rise time of 120 ns, which demonstrates that the sensor is capable of observing the dynamics of the pressure transient during a blast event.

Keywords: pressure sensor, fiber optic, traumatic brain injury, shock tube

(Some figures may appear in colour only in the online journal)

1. Introduction

Traumatic brain injury (TBI) [1–3] caused by a soldier's exposure to an explosive event can be difficult to diagnose. To effectively study the brain injury mechanism, it is critical to accurately measure the pressure of a blast wave and its effect on the human body [4–8]. A blast wave in air includes a shock wave, which is a nearly instantaneous rise in pressure, temperature and density, which propagates outward from the explosion at a rate greater than the speed of sound. Pressure sensors featuring a fast dynamic response are required in these studies to measure the rapid pressure changes in the shock wave. An ideal pressure sensor for a blast event measurement needs to respond very quickly, be compact, not interfere with the propagating blast wave and should be able to measure with high spatial resolution. Currently, most pressure transducers are piezo-electrical based which usually suffer from low spatial resolution because of the bulky size. The cross-sensitivity from the acceleration may be another issue for piezo-electrical pressure sensor. On the other hand, due to the fast dynamic response, miniature size, simple structure and immunity to electro-magnetic interference (EMI), fiber optic

pressure sensors are potential substitutes for piezo-electrical transducers. The most commonly used fiber optic pressure sensor structure utilizes the Fabry–Perot (FP) structure [9–15]. The FP cavity is formed by attaching a diaphragm, which is used as a sensing element, to a hollow core supporting structure. Despite the simplicity of the FP structure, the resonant frequency of the diaphragm can be tailored by changing the material and the mechanical parameters of the diaphragm. The low mass of the diaphragm and the fiber reduces the sensor's mass loading and does not significantly affect the inertial response or the mechanical stiffness of the structure to which the sensor is attached.

Several groups are working on applying fiber optic pressure sensors to measure the shock wave in a blast event. The fiber optic pressure sensor fabricated by MacPherson *et al* was tested in a blast event [16]. A well-cleaved optical fiber was inserted into a ferrule and a copper diaphragm was bonded at the end surface of the ferrule. An FP cavity was formed between the fiber tip and the diaphragm. The sensor was tested in a blast event and was compared with other sensors. The sensor showed a rise time of 3 μs with a dynamic range of 100 kPa. In another paper published by the same group in 2006 [17], an FP cavity was formed by bonding a 1 μm thickness silicon dioxide diaphragm to a pre-etched silicon supporting structure. The rise time of the sensor was shown to be less than 4 μs under a pressure range up to 8 kPa. Similar work was done by Parkes *et al* in 2007 [18]. In their paper, silicon dioxide and silicon nitride were used to fabricate the diaphragm and the results of the different diaphragms in a transient pressure measurement were compared. Sensors made with both of the diaphragms could achieve a rise time of 3 μs with a range from 0.1 MPa to 1 MPa. Chavko *et al* measured the shock wave in a rat brain by using a fiber optic pressure sensor made by FISO Technologies (Quebec, Canada) [6]. The results indicated that the shock wave in the rat brain has a rise time of at least 0.4 ms from 0 to 50 kPa. In these papers, FP structures were fabricated by bonding diaphragms to external supporting structures. Such configurations use bulky sensor heads so that the spatial resolution is limited. Furthermore, attaching external supporting structures to the optical fiber using bonding materials, such as glue or epoxy, is not a reliable method because of the unstable and inconsistent properties of the bonding materials.

Blast event measurements for TBI studies require sensors to have a fast response and ideally a point or at least a compact measurement. The thickness and the diameter of the diaphragm limit the resonant frequency of the sensor. The dimension of the sensor determines if the sensor can be utilized for point measurements. Conventional FP structure fabrication methods cannot control the thickness of the diaphragm precisely [9–13]. In these methods, the thickness of the diaphragm is controlled by cleaving the optical fiber by the operators which cannot be precisely controlled. The authors have previously reported that using the microelectromechanical systems (MEMS) technique to fabricate the silicon dioxide diaphragm separately and then thermally bonding it with a fiber is a promising way to tailor the resonant frequency of the sensor based on an FP structure [15]. The accurately controlled diaphragm thickness and diameter promise dynamic response of the sensor. In this paper, a miniature ultra-fast fiber optic pressure sensor was designed and fabricated for the purpose of quantifying the physics of a blast wave by measuring the transient pressure change in a blast event. The sensor is based on the FP interferometer principle. The diameter of the sensor is the same as that of the optical fiber, which is generally 125 μm. Such compact designs allow for a high degree of sensor spatial resolution during a blast event measurement. The silicon dioxide diaphragm that is used as the sensing element is made separately by the MEMS technique which can control the thickness of the diaphragm very precisely. The diaphragm is thermally bonded on the end face of the optical fiber. The results published in the previous literature have demonstrated that the sensor has the capabilities of low hysteresis and linear sensitivity [15]. In order to increase the sensor's resonant frequency, the mechanical properties of the diaphragm were designed carefully so that the sensor can be fast enough for capturing the rapid pressure change in the blast event. The dynamic properties of the sensor were characterized in a shock tube experiment side by side with a commercially available reference sensor. The shock tube test showed that the new fiber optic sensor features an ultra-fast response with a rise time of 120 ns with the lowest resonant frequency at approximately 4.12 MHz.

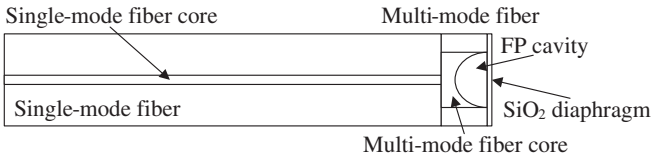

Figure 1. Schematic diagram of the fiber optic pressure sensor. The sensor consists of three parts: a SMF, a MMF and a silicon dioxide diaphragm. The FP cavity is fabricated by wet etching away the core of the MMF. The diaphragm is the sensing element.

2. Sensor design and fabrication

The fiber optic pressure sensor is based on the FP principle. A schematic diagram of the sensor is shown in figure 1. The sensor consists of three parts: a single-mode fiber (SMF), a multi-mode fiber (MMF) and a silicon dioxide diaphragm with controllable thickness. The SMF is used for propagating the light and illuminating the MMF with the diaphragm. An FP cavity is fabricated along the axis of the MMF by wet etching away the core. A silicon dioxide diaphragm is thermally bonded on the end face of the wet-etched MMF to form a FP structure that can sense the outside pressure change. There is no bulky sensing element required by using this structure, which means the sensor maintains a compact size by keeping the sensing element the same dimension as the optical fiber.

When an incident light illuminates the FP structure, the light reflects on two interfaces: one is between the MMF core and the FP cavity; the other one is between the FP cavity and the silicon dioxide diaphragm. The two reflections interfere with each other and will generate an interference pattern. The interference pattern will shift according to the change of the distance between the two interfaces, which is called the FP cavity length. By interrogating the interference pattern shift

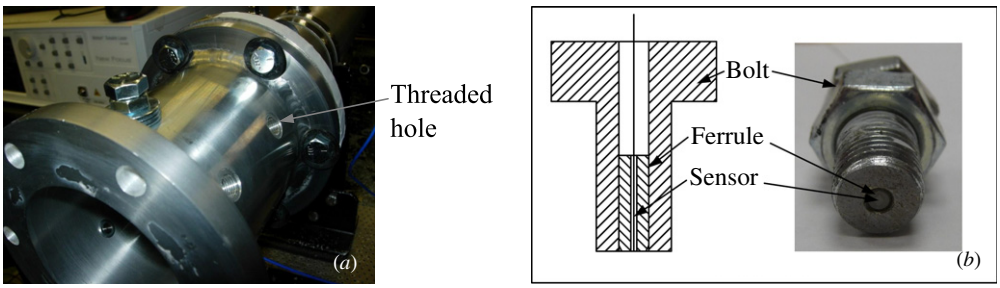

Figure 2. (*a*) A threaded hole is used to mount the sensor on the shock tube. (*b*) Schematic design of the sensor package and photograph of the real sensor package.

corresponding to the change of the FP cavity length caused by the pressure-induced diaphragm deformation, the pressure information can be obtained.

The method of fabrication is published in the previous paper [15]. Briefly, the silicon dioxide diaphragm was prepared by back etching away the silicon on a silicon wafer with a 3 μm oxide layer by deep reactive ion etching (RIE). The thickness of the diaphragm can be customized by choosing different thickness of the oxide layer grown on the silicon wafer. The MMF and the SMF was fusion spliced together, followed by cleaving the MMF and leaving the length of the MMF to be 20–40 μm. The spliced optical fiber was immersed in 49% hydrofluoric acid (HF) for 3 min to etch away the MMF core. The faster etching rate of the core than that of the cladding ensures that the MMF core can be etched away without damaging the cladding. After the wet etching, the fiber was moved to a 3-axis stage in order to align with the diaphragm. The bonding was performed by heating both the fiber and the diaphragm with a propane torch.

One of the advantages in fabricating the diaphragm separately by MEMS is that the performance of the fiber optic pressure sensor can be highly predicted by tailoring the thickness of the diaphragm precisely. Due to this fabrication method, the performances of the sensor, such as the sensitivity and the resonant frequency, are predictable and can be customized in the design step according to different applications. Furthermore, the MEMS technique promises uniformity and quality of the diaphragm in one batch, which opens a way to mass production capability. Meanwhile, by bonding the diaphragm directly onto the etched optical fiber, the sensor is very small and compact without a bulky head.

In order to achieve a high resonant frequency so that the fiber optic sensor could have a fast response to the shock wave, the dimension of the silicon dioxide diaphragm was designed carefully. The resonant frequency of the sensor is dependent on the diameter of the sensing area, the thickness of the diaphragm and the material of the diaphragm [12]. For a given material and a given diameter of the sensing area, the lowest resonant frequency is proportional to the thickness. On the other hand, the deformation of the diaphragm under a certain pressure is inversely proportional to the third power of thickness. Increasing the thickness of the diaphragm leads to the increment of the lowest resonant frequency at the expense of decreased sensitivity. In this design, the material of the diaphragm was chosen as silicon dioxide which could be bonded perfectly with the optical fiber by using the thermal bonding technique. The diameter of the sensing area on the diaphragm was measured at 68.4 μm. The thickness of the diaphragm was 3 μm. Therefore, the lowest resonant frequency was calculated to be 4.113 MHz according to the formula in reference [12]. Having such a frequency enables a fast rise time while maintaining a relatively high sensitivity. The actual resonant frequency and the rise time were characterized in a shock tube experiment to verify the sensor design.

3. Sensor package

Prior to the shock tube experiment, a package was designed to protect the sensor and to mount the sensor on the shock tube. There were two threaded holes on the side wall of the shock tube that were used to screw the sensors in as shown in figure 2(*a*). In order to mount the sensor on the shock tube securely, a bolt that can mate the threaded hole was drilled in the center to place the sensor as shown in figure 2(*b*). A ferrule with an inner diameter of 127 μm was placed inside the hole to hold the sensor. The sensor was glued in the ferrule with epoxy. The bottom surfaces of the bolt, the ferrule and the sensor were adjusted to sit flush with the shock tube interior surface.

4. Shock wave measurement

4.1. Light intensity interrogation

In the previous sensor verification experiments, the sensors have demonstrated good linearity, high sensitivity and low hysteresis [15]. However, the interrogation method used in the static experiments was slow. The fiber optic sensor was interrogated by obtaining the reflection interference pattern within a specific wavelength range. By using this interrogation method, the full spectrum of the sensor should be retrieved which makes this method very slow because the capability of processing the huge amount of data in a short time is very limited. In fact, the instrument that was used to interrogate the fiber optic pressure sensor previously sampled data at 5 Hz. It is not fast enough to capture the rapid changing pressure in a shock wave measurement. Therefore, in the blast wave measurement application where a fast interrogation method is needed, the interference pattern interrogation approach is substituted by the light intensity interrogation approach.

The principle of the light intensity interrogation approach is illustrated in figure 3. Two plots in the figure demonstrate

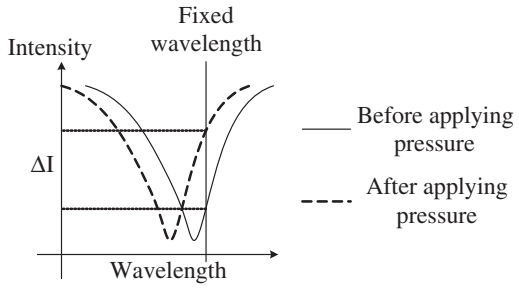

Figure 3. Principle of the light intensity interrogation approach. As the interference pattern shifts, the intensity of the reflection at a specific fixed wavelength is changed. The amount of the intensity change corresponds to how much the interference pattern shifts.

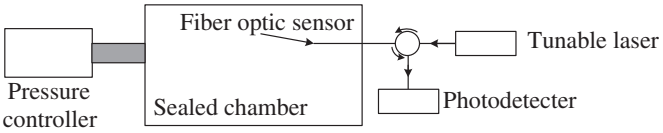

Figure 4. Schematic diagram of the calibration system. A tunable laser was used to excite the fiber optic sensor with a specific wavelength of laser. The intensity of the reflection was measured by a photodetector and the data were transferred to a PC through a DAQ.

the interference pattern before the pressure is applied and after the pressure is applied, respectively [15]. The dashed line indicates the interference pattern after the pressure is applied. Generally, the amount of interference pattern shift could be calculated by the difference of the valley wavelengths. If a photodetector is used to observe the light intensity at a specific single wavelength, which is referred to as 'fixed wavelength' in figure 3, as the interference pattern is shifting to the left, the photodetector would observe a light intensity increase. The relationship between the light intensity change and the interference pattern shift is described in the previous literature [19]. Because of the wide bandwidth of the photodetector, the light intensity interrogation method has the capability of tracking fast changing pressures in the blast event by choosing the proper data acquisition (DAQ) system.

4.2. Sensor calibration setup

Prior to measuring the shock wave in the blast event, the fiber optic pressure sensor needs to be calibrated in order to obtain the relationship between the output of the photodetector and the pressure. A schematic diagram of the calibration system is shown in figure 4. The fiber optic pressure sensor was placed in a sealed chamber in which the pressure was controlled precisely by a pressure controller (NetScanner Model 9034, Pressure Systems Inc.) at room temperature. A tunable laser (NewFocus TLB-6600, Newport) was used to excite the fiber optic sensor with a specific wavelength of the laser. The intensity of the reflection was measured by a photodetector (PDA10CS, Thorlabs). The data were transferred to a PC through a DAQ system (M2i.4032, Spectrum GmbH). The pressure in the chamber was first increased in increments and then decreased in the same manner. The increasing and decreasing cycle was repeated three times in order to evaluate the sensor's repeatability.

4.3. Shock tube experiment setup

Figure 5 shows a photograph and a schematic diagram of the shock wave measurement experiment setup. A chamber made of aluminum was attached to the end of the shock tube located at Natick Soldier Research, Development and Engineering Center (NSRDEC) in Natick, MA. A fiber optic pressure sensor was used in the experiment as well as a reference sensor (Model# 102B06, PCB Piezotronics, Inc.). The fiber optic sensor and the reference sensor were mounted facing each other at the same longitudinal position in order to obtain the propagating shock waves simultaneously. The fiber optic sensor was interrogated by the light intensity interrogation method mentioned above and both signals from the fiber optic sensor and the reference sensor were sampled by a PC using the DAQ system (M2i.4032, Spectrum GmbH). The sampling rate of the DAQ system was set to 50 MHz.

5. Results and discussions

5.1. Calibration results

Before the fiber optic sensor was calibrated, the reflection interference spectrum of the fiber optic pressure sensor was obtained by an optical sensing analyzer (OSA) (Si720, Micron Optics, Inc.) in order to determine which working wavelength of the tunable laser should be chosen. The spectrum is shown in figure 6. According to the figure, the working wavelength of the tunable laser in the light intensity interrogation method

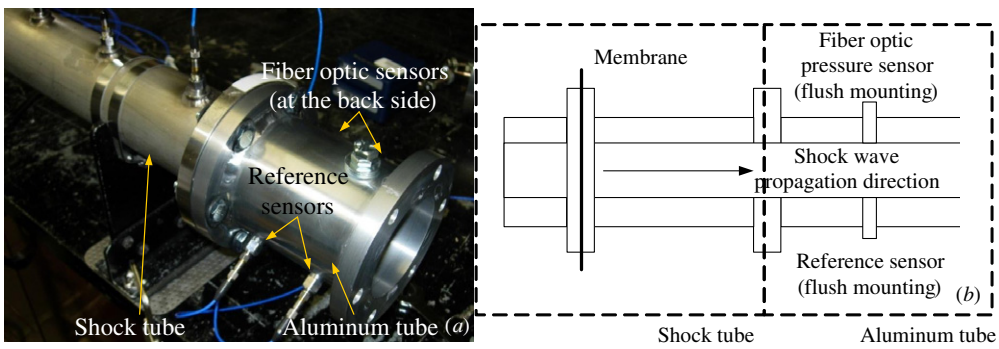

Figure 5. (*a*) Photograph of the experiment setup. An aluminum tube was attached to the end of the shock tube. (*b*) Schematic diagram (not to scale) of the shock wave measurement experiment setup. A fiber optic pressure sensor and a reference sensor were mounted face to face at the same position in order to measure the propagating shock wave simultaneously.

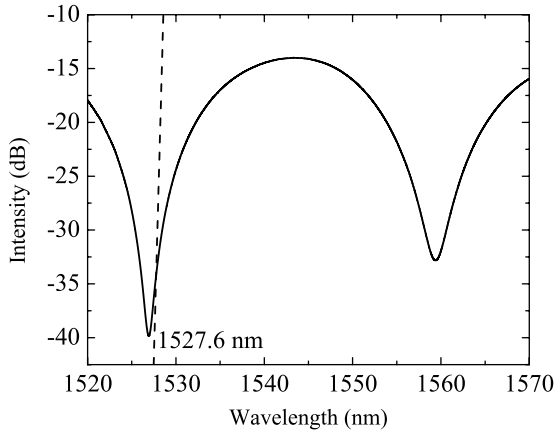

Figure 6. The reflection interference spectra of the fiber optic pressure sensor. The working wavelength of the tunable laser in the light intensity interrogation method was chosen at 1527.6 nm.

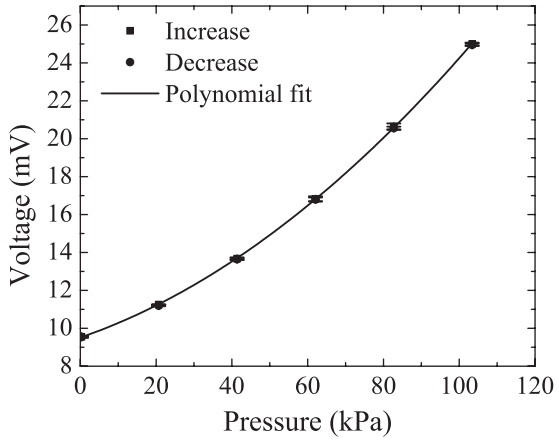

Figure 7. The calibration result of the fiber optic pressure sensor. The voltage from the photodetector increased corresponding to the pressure increase.

was chosen at 1527.6 nm. The working wavelength was chosen at the point where the maximum slope in the spectrum was estimated in order to achieve the highest sensitivity.

The calibration results are illustrated in figure 7. The pressure range was from 0 to 103.4 kPa (15 psi). The pressure in the experiment chamber was increased in steps with each increment step being 20.68 kPa (3 psi). The pressure was subsequently decreased using the same increments. The procedure was repeated three times in order to evaluate the sensor's repeatability. In the figure, the squares and the dots represent the mean value of the increasing cycles and the decreasing cycles, respectively. From the figure it can be clearly seen that the standard deviations of the increasing and decreasing cycles are small and each square and dot overlap with each other which means that the sensor's repeatability is very good and the hysteresis is very low. A second order polynomial fit was performed for the data due to the nonlinearity of the sensor's response to the pressure. The polynomial function can be described as $y = A + B_1x + B_2x^2$, where $A = 9.512$, $B_1 = 0.069$ and $B_2 = 7.846 \times 10^{-4}$, respectively. The adjusted R-square coefficient is calculated to be 0.999. The sensitivity is calculated as $B_1 + 2B_2x$. The resolution of the measured sensor is different within different pressure ranges due to the sensor's nonlinearity. According to the datasheet of the photodetector and the resolution of the DAQ system, the worst resolution is calculated to be 1.406 kPa. Because the measured intensity at the selected working wavelength will change the behavior if the interference spectrum in figure 6 shifts beyond a quarter period, the working pressure range of the measured sensor is calculated to be 579.439 kPa.

Nonlinearity can be observed in figure 7. The nonlinearity of the fiber optic pressure sensor is due to the varying slope of the sensor's spectrum. As the pressure increases, the reflection interference spectrum of the sensor shifts to the left linearly [15]. The amount of the spectrum shift is related to the linear pressure change. However, due to the nonlinearity of the region where the working wavelength was chosen, the relationship between the output voltage and the pressure was not linear. Furthermore, note that in figure 6, the unit of the intensity is in decibels, which means that even if the working region was linear, the output from the photodetector might not be linear because the photodetector responds to the optical intensity linearly. A lookup table (LUT) can be used to store the voltage–pressure pairs in order to compensate the nonlinearity after the calibration.

5.2. Capability of capturing shock waves

After the shock waves were generated in the shock tube, there were multiple peaks due to the multiple reflections along the shock tube and the aluminum chamber. Figure 8 shows the first cycle of the shock waves that was captured by the fiber optic sensor and the reference sensor. The gain of the photodetector was set to 10 dB. Figure 8(*a*) shows the shock wave profile in the time period of −1 to 8 ms. Figure 8(*b*) shows the time zoom-in data of figure 8(*a*). The time scale is from 0 to 1 ms.

From the figures, it can be seen that the fiber optic sensor showed the capability of capturing the rapidly changing shock wave profile. The signal from the fiber optic sensor was similar to the one from the reference sensor including the rise part and the decay part. It should be noticed that the difference between the *Y*-scales in the figures is due to the different sensitivities of the sensors. The areas highlighted by circles in figure 8(*b*) show that the resonant frequencies of the fiber optic sensor's diaphragm were excited by the shock wave.

5.3. Resonant frequencies of the sensor

The resonant frequency of the sensor determines the limitation of the maximum frequency of the signal that the sensor can measure. According to a rule of thumb for the resonant pressure sensor, the maximum frequency of the signal is 0.2 of the resonant frequency of the sensor [17]. In order to investigate the sensor's resonant frequencies, the signal from the fiber optic sensor with the time period from 110 to 150 μs was considered. The signal is shown in figure 9(*a*). After performing a fast Fourier transform (FFT), the frequency domain results are illustrated in figure 9(*b*). There are two resonant frequencies that were excited. One is at 4.12 MHz

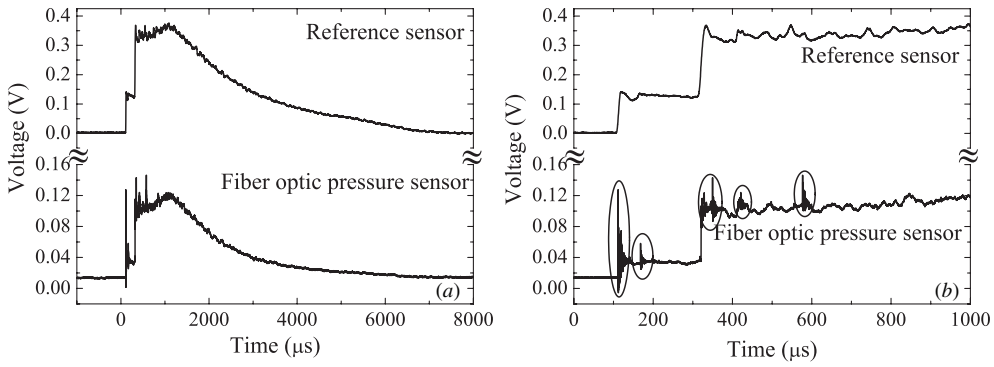

Figure 8. The shock wave profile that was captured by the fiber optic sensor and the reference sensor. (*a*) The shock wave profile from −1 to 8 ms. (*b*) The time zoom-in shock wave profile from 0 to 1 ms.

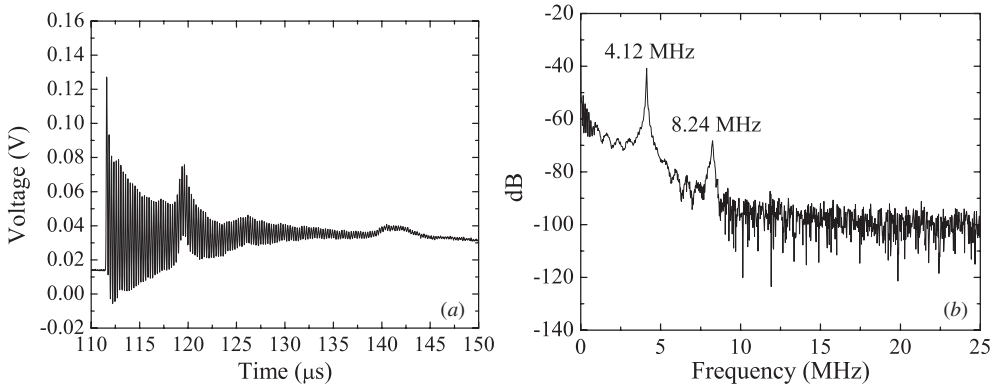

Figure 9. Evaluation of sensor's resonant frequencies. (*a*) The signal segment that was used for evaluation. The time period is from 110 to 150 μs. (*b*) The frequency domain results after performing FFT.

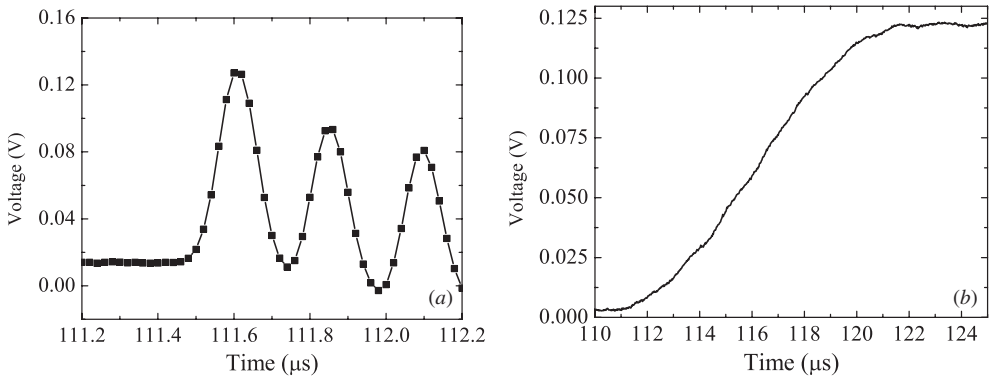

Figure 10. The rise time comparison. (*a*) The signal from the fiber optic sensor at the first rise part indicates that it features a rise time of 120 ns. (*b*) The signal from the reference sensor at the same first rise part showed that the reference sensor has a rise time of approximately 10 μs.

and the other one is at 8.24 MHz. According to the formula in reference [12], which is

$$f_{00} = \frac{\alpha_{00}}{4\pi}\left[\frac{E}{3w(1-\mu^2)}\right]^{1/2}\left(\frac{h}{r^2}\right)$$

where f_{00} is the lowest resonant frequency; α_{00} is a constant related to the vibrating modes, which is 10.21 for the lowest natural frequency; E is Young's modulus and μ is the Poisson ratio; w is the mass density of the material; and r and h are the radius and the thickness of the diaphragm, respectively. Since the material of the diaphragm is silicon dioxide, Young's modulus, the Poisson ratio and the mass density are chosen. The lowest resonant frequency is determined by the thickness and the radius of the diaphragm. The thickness of the reported diaphragm is 3 μm due to the thickness of the oxide layer on the purchased silicon wafer. The diameter of the diaphragm was measured to be 68.4 μm after the fabrication. Therefore, the theoretical lowest resonant frequency was calculated to be 4.113 MHz which is similar to the experimental result. Such resonant frequency allows the data with the maximum frequency component of 824 kHz to be captured.

5.4. Rise time of the sensor

In order to determine the rise time of the fiber optic sensor, the signal from the fiber optic sensor was extracted between

111.2 μs and 112.2 μs and it is shown in figure 10(*a*). This period of the signal indicates the first rise part. For the purpose of comparison, the first rise part of the signal from the reference sensor is shown in figure 10(*b*). The reference sensor showed the rise time of approximately 10 μs which matches the rise time mentioned in the datasheet. It has to be noted that the rise time of the fiber optic pressure sensor was observed with the presence of resonance. In most practical applications, the resonance should be avoided in order to take an accurate measurement. In these cases, the bandwidth of the signal that is measured by the sensor will be limited.

6. Conclusions

This paper presents an ultra-fast fiber optic pressure sensor that can be used to measure the rapidly changing pressure in a blast event. The principle of the sensor is the FP interferometer. The sensor was fabricated by splicing a specific length of MMF with a piece of SMF followed by etching away the core of the MMF. A piece of silicon dioxide was thermally bonded on the end surface of the pre-etched MMF which serves as a sensing element. The thickness of the diaphragm was chosen to be 3 μm allowing the sensor to have a fast response while still maintaining good sensitivity. The outer diameter of the sensor is 125 μm which further promises that the sensor can feature high spatial resolution. The lowest resonant frequency of the sensor was tailored at 4.113 MHz after design.

A shock tube experiment was performed in Natick Soldier Research, Development and Engineering Center (NSRDEC) in Natick, MA. A special package was designed to protect the sensor and to mount the sensor. In the experiment, the signal from the fiber optic sensor matched with that from the reference sensor quite well. The experiment also demonstrated that the fiber optic sensor exhibits the lowest resonant frequency at 4.12 MHz. Furthermore, the experiment illustrates that the fiber optic sensor features a rise time of 120 ns compared to 10 μs of the reference sensor.

Acknowledgments

The authors are grateful for the collaboration with Natick Soldier Research, Development and Engineering Center for sharing the shock tube and the reference pressure sensors. The authors also appreciate the Army Research Laboratory for sponsoring this work (Nanomanufacturing of Multifunctional Sensors Award Number W911NF-07-2-0081).

References

[1] Okie S 2005 Traumatic brain injury in the war zone *N. Engl. J. Med.* **352** 2043–7

[2] DePalma R G, Burris D G, Champion H R and Hodgson M J 2005 Blast injuries *N. Engl. J. Med.* **352** 1335–42

[3] Wightman J M and Gladish S L 2001 Explosions and blast injuries *Ann. Emerg. Med.* **37** 664–78

[4] Taber K H, Warden D L and Hurley R A 2006 Blast-related traumatic brain injury: what is known? *J. Neuropsychiatry Clin. Neurosci.* **18** 141–5

[5] Povlishock J T and Katz D I 2005 Update of neuropathology and neurological recovery after traumatic brain injury *J Head Trauma Rehabil.* **20** 76–94

[6] Chavko M, Koller W A, Prusaczyk K W and McCarron R M 2007 Measurement of blast wave by a miniature fiber optic pressure transducer in the rat brain *J. Neurosci. Methods* **159** 277–81

[7] Irwin R J, Lerner M R, Bealer J F, Mantor C P, Brackett D J and Tuggle D W 1999 Shock after blast wave injury is caused by a vagally mediated reflex *J Trauma* **47** 105–10

[8] Moochhala S M, Shirhan Md, Jia Lu, Teng C-H and Greengrass C 2004 Neuroprotective role of aminoguanidine in behavioral changes after blast injury *J. Trauma* **56** 393–403

[9] Wang A, Xiao H, Wang J, Wang Z, Zhao W and May R G 2001 Self-calibrated interferometric-intensity-based optical fiber sensors *J. Lightwave. Technol.* **19** 1495

[10] Wang X, Xu J, Zhu Y, Cooper K L and Wang A 2006 All-fused-silica miniature optical fiber tip pressure sensor *Opt. Lett.* **31** 885–7

[11] Xu J, Pickrell G, Wang X, Peng W, Cooper K and Wang A 2005 A novel temperature-insensitive optical fiber pressure sensor for harsh environments *IEEE Photonics Technol. Lett.* **17** 870–2

[12] Xu J, Wang X, Cooper K L and Wang A 2005 Miniature all-silica fiber optic pressure and acoustic sensors *Opt. Lett.* **30** 3269–71

[13] Zhu Y and Wang A 2005 Miniature fiber-optic pressure sensor *IEEE Photonics Technol. Lett.* **17** 447–9

[14] Wang W, Wu N, Tian Y, Wang X, Niezrecki C and Chen J 2009 Optical pressure/acoustic sensor with precise Fabry–Perot cavity length control using angle polished fiber *Opt. Express* **17** 16613–8

[15] Wang W, Wu N, Tian Y, Niezrecki C and Wang X 2010 Miniature all-silica optical fiber pressure sensor with an ultrathin uniform diaphragm *Opt. Express* **18** 9006–14

[16] MacPherson W N, Gander M J, Barton J S, Jones J D C, Owen C L, Watson A J and Allen R M 2000 Blast-pressure measurement with a high-bandwidth fibre optic pressure sensor *Meas. Sci. Technol.* **11** 95

[17] Watson S, MacPherson W N, Barton J S, Jones J D C, Tyas A, Pichugin A V, Hindle A, Parkes W, Dunare C and Stevenson T 2006 Investigation of shock waves in explosive blasts using fibre optic pressure sensors *Meas. Sci. Technol.* **17** 1337

[18] Parkes W, Djakov V, Barton J S, Watson S, MacPherson W N, Stevenson J T M and Dunare C C 2007 Design and fabrication of dielectric diaphragm pressure sensors for applications to shock wave measurement in air *J. Micromech. Microeng.* **17** 1334

[19] Wu N, Wang W, Ling Y, Farris L, Kim B, McDonald M J and Wang X 2010 Label-free detection of biomolecules using LED technology *Proc. SPIE* **7574** 75740I